ment (Fig. 1C). If +25 and Δ23 recombined to yield a functional TK gene, a recombinant 720-bp fragment representing the 5′ end of a functional gene should be generated. In this instance, a double-deletion gene formed by the reciprocal recombination event should generate a 5590-bp band (Fig. 1B). In the lanes that have DNA from cell lines generated by mixtures of +25 and Δ23, the 720-bp fragment representative of recombination is present. The 5590-bp fragment is visualized in three of the five cell lines.

These data indicate that recombination between homologous genes occurred during DNA-mediated gene transfer and that the recombination events restored the function of mutant genes at high frequency. For example, the number of TK^+ colonies was 10 percent of the number generated by a wild-type TK gene. Our data do not permit a distinction between classical homologous recombination, as seen in bacteria and yeast (*1–4*), and gene conversion, which also occurs in yeast (*18*) and perhaps in mammalian cells (*19*). Although there are differences between the two mechanisms, both depend on homology between two regions of DNA. In either case, the high frequency with which two homologous genes can undergo recombination suggests that integration of exogenous genes into the recipient cell genome may also occur at sites of homology at a detectable frequency.

JUDY SMALL
GEORGE SCANGOS*

Department of Biology,
Johns Hopkins University,
Baltimore, Maryland 21218

References and Notes

1. M. S. Fox and M. K. Allen, *Proc. Natl. Acad. Sci. U.S.A.* **52**, 412 (1964); T. Gurney, Jr., and M. S. Fox, *J. Mol. Biol.* **32**, 83 (1971); R. D. Hotchkiss and M. Gabor, *Annu. Rev. Genetics* **4**, 193 (1970).
2. D. T. Stinchcomb, K. Struhl, R. W. Davis, *Nature (London)* **282**, 39 (1979).
3. K. Struhl, D. T. Stinchcomb, S. Scherer, R. W. Davis, *Proc. Natl. Acad. Sci. U.S.A.* **76**, 1035 (1979).
4. A. Hinnen, J. B. Hicks, G. R. Fink, *ibid.* **75**, 1929 (1978).
5. A. Pellicer, M. Wigler, R. Axel, S. Silverstein, *Cell* **14**, 133 (1978).
6. M. Wigler, A. Pellicer, S. Silverstein, R. Axel, *ibid.*, p. 725.
7. A. Pellicer *et al.*, *Science* **209**, 1414 (1980).
8. G. Scangos, K. M. Huttner, D. K. Juricek, F. H. Ruddle, *Mol. Cell. Biol.* **1**, 111 (1981).
9. G. Scangos and F. H. Ruddle, *Gene* **14**, 1 (1981).
10. R. Holliday, *Symp. Soc. Gen. Microbiol.* **20**, 359 (1970).
11. H. Gruneberg, *Genet. Res.* **7**, 58 (1962).
12. S. A. Latt, *Proc. Natl. Acad. Sci. U.S.A.* **71**, 3162 (1974).
13. C. Brack, M. Hirama, R. Lenhard-Schuller, S. Tonegawa, *Cell* **15**, 1 (1978).
14. D. A. Jackson, in *Introduction of Macromolecules into Viable Mammalian Cells*, R. Baserga, C. Croce, G. Rovera, Eds. (Liss, New York, 1980), p. 65; C. T. Wake and J. H. Wilson. *Proc. Natl. Acad. Sci. U.S.A.* **76**, 2876 (1979); P. Upcroft, B. Carter, C. Kidson, *Nucleic Acids Res.* **8**, 5835 (1980).
15. P. J. Kretschmer, A. H. Bowman, M. H. Huberman, L. Sanders-Haigh, L. Killos, W. F. Anderson, *Nucleic Acids Res.* **9**, 6199 (1981); R. A. Anderson, T. Krakauer, R. D. Camerini-Otero. *Proc. Natl. Acad. Sci. U.S.A.* **79**, 2748 (1982).
16. S. L. McKnight, E. R. Gavis, R. Kingsbury, R. Axel, *Cell* **25**, 385 (1981).
17. E. Southern, *J. Mol. Biol.* **98**, 503 (1975).
18. S. Fogel and R. Mortimer, *Proc. Natl. Acad. Sci. U.S.A.* **62**, 96 (1969).
19. J. M. Roberts and R. Axel, *Cell* **29**, 109 (1982).
20. K. M. Huttner, J. A. Barbosa, G. Scangos, D. Prautcheva, F. H. Ruddle, *J. Cell Biol.* **91**, 153 (1981).
21. E. H. Szybalska and W. Szybalski, *Proc. Natl. Acad. Sci. U.S.A.* **48**, 2026 (1962); J. W. Littlefield, *Science* **145**, 709 (1964).
22. B. Christy and G. Scangos, *Proc. Natl. Acad. Sci. U.S.A.* **79**, 6299 (1982).
23. We thank S. L. McKnight for the −109 and +25 plasmids, E. Fyrberg and D. Powers for critical evaluation of the manuscript, G. Ketner for helpful suggestions, and D. Warr for manuscript preparation. This work was supported by NSF award PCM8105296. J.S. was supported by NIH predoctoral training grant GM 5T32 GM07231-08. This is contribution number 1187 from the Department of Biology.
* To whom all correspondence should be addressed.

13 September 1982; revised 28 October 1982

Quaternary and Quinternary Structures of Native Chromatin DNA in Liver Nuclei: Differential Scanning Calorimetry

Abstract. *Differential scanning calorimetry of chromatin isolated from rat liver cells revealed three discrete thermal transitions whose temperatures and melting enthalpies depend on ionic strength in the range 0 to 600 millimolar NaCl. Intact nuclei showed a fourth thermal transition at a lower temperature and different melting enthalpies for the other three transitions still present at temperatures similar to those obtained in isolated chromatin. The data are discussed in terms of the tertiary, quaternary, and quinternary structures of chromatin DNA.*

Although it is generally agreed that the basic chromatin DNA fiber (tertiary structure) is about 110 Å in diameter and is composed of closely apposed nucleosomes (*1*), experimental findings have led to several models for the higher order structure in native chromatin (*2–6*) during interphase. We present detailed evidence on the levels of higher order chromatin structure obtained by means of a recently developed nondestructive biophysical probe.

The study of the dependence of the optical properties of biological macromolecules on temperature is a current method of identifying their discrete conformational states, and it provides indirect information on the thermodynamics of the transitions (*6–8*). However, this approach has serious limitations (*6–8*).

Using a sensitive differential scanning calorimeter (Perkin-Elmer, DSC II), we have begun a systematic study of enthalpy changes versus temperature for both chromatin and intact nuclei in a range of ionic strengths far greater than the 7 m*M* limit possible with traditional spectrophotometry or spectropolarimetry. Thermal profiles of nuclei had up to now been prohibitive not only because of their relatively high physiological strength, but also because of their high sedimentation and light scattering. With calorimetry, it is possible to study the stability of the DNA and its higher order structures "in situ."

Figure 1 shows the heat capacity (dq/dT) versus temperature, in the range 300 to 400 K, for isolated chromatin in 1 m*M* tris-HCl, *p*H 8, at 0, 10, 50, and 600 m*M* NaCl. Three transitions (I, II, and III), whose temperature values change slightly with salt concentration, are clearly and reproducibly identifiable. As shown in Fig. 1 and summarized in Fig. 2, the enthalpy change (ΔH) for isolated chromatin varies with salt concentration; the enthalpy change decreases between 0 and 10 m*M* and then remains constant for transition I, increases steadily for transition III, and increases sharply up to 50 m*M* and then decreases sharply at 600 m*M* for transition II.

Table 1. Temperatures of thermal transitions determined by circular dichroism measurements at 272 nm (DNA conformation) and 223 nm (protein conformation). The peak value is taken from the derivative plot of the temperature-dependent measurements (*7, 10*). T_S (negative derivative) and T_M (positive derivative) represent, respectively, the superhelix-helix and helix-coil transitions as determined by the molar ellipticity at 272 nm. T_P represents the position of the only peak in the derivative plot of the molar ellipticity at 223 nm. Ellipticity and absorbancy, at given wavelength, were measured on our modified J-40 spectropolarimeter equipped with both circulatory bath and PG-VL thermostat (*8*). At 1 to 7 m*M* tris-HCl, an abrupt decrease in molar ellipticity could be monitored at 272 nm, even if the thermal transition was not completed by 367 K; at higher ionic strengths, this decrease was not apparent.

Sample	Temperature (°K)		
	T_M	T_S	T_P
Protein-free DNA at 1 m*M* tris	~ 333		
Protein-free DNA at 50 m*M* NaCl	~ 355		
Chromatin at 1 m*M* tris	> 367	~ 360	~ 345

To better identify the various enthalpy transitions, we obtained parallel melting curves on a similar chromatin sample at 1 m*M* tris-HCl (Table 1), using absorbance where DNA helix-coil and superhelix-helix cannot be discriminated because both yield hyperchromatic effects (*8*), and circular dichroism at 272 nm where the two transitions can be discriminated because of their opposite sign in molar ellipticity (*7–10*). At ionic strengths greater than a few millimoles per liter, chromatin not only displays a melting temperature above 95°C, but tends to shrink and aggregate, preventing optical characterization.

A derivative plot of chromatin molar ellipticity at 272 nm versus temperature [Table 1 and (*7*)] at 1 m*M* tris allows several conformational transitions to be identified and compared to the enthalpy transitions observed by microcalorimetry on similar 1 m*M* tris chromatin (Fig. 1). One transition above 367 K is characterized by a decrease in molar ellipticity (negative derivative) and a pronounced increase in absorbance and is thereby related to the helix-coil conformational transition (*7, 10*); it may correspond only to transition III in the heat capacity profile (Fig. 1). One at around 360 K is characterized by an increase in molar ellipticity and is apparently related to the so-called superhelix-to-helix transition (*9, 10*); it appears to correspond to transition II in the heat capacity profile (Figs. 1 and 2).

The changes in chromatin condensation (not shown) closely parallel changes with ionic strength in ΔH for transition II. This further corroborates the assignment of transition II to a transition from a quaternary to a lower order superpacking of chromatin DNA. Monitoring the temperature dependence of molar ellipticity at 223 nm, which mainly reflects changes in protein structure, and the use of a subsequent derivative plot reveal a sharp transition at about 345 K [see also (*6*)], which corresponds strikingly to the first heat capacity transition (transition I) (Figs. 1 and 2). While transition enthalpies are strongly dependent on ionic strength, transition temperatures appear to be only slightly (if at all) dependent on ionic strength at 0, 10, 30, 50, 100 (intact nuclei), and 600 m*M* NaCl.

The melting of protein-free DNA is strongly dependent on ionic strength, being about 333 K at 1 m*M* tris and about 355 K at 50 m*M* NaCl, with only one broad thermal transition in the heat capacity profile (not shown). In our native chromatin preparation, however, no DNA is in such a protein-free condition, as shown by the electron microscopy in the same sample (*12*) and suggested by the lack of any thermal transition below 345 K at 1 m*M* tris in both the heat capacity (Fig. 1) and absorbance–circular dichroism (Table 1) profiles.

The effect of a 600 m*M* NaCl wash, which removes the H1 histone from chromatin and disrupts the quaternary structure, combined with the critical ΔH dependence on ionic strength—expected also from polyelectrolyte theory (*11*)—is compatible with the possible assignment of transition II to the quaternary structure (*2, 3, 12*). The melting temperature

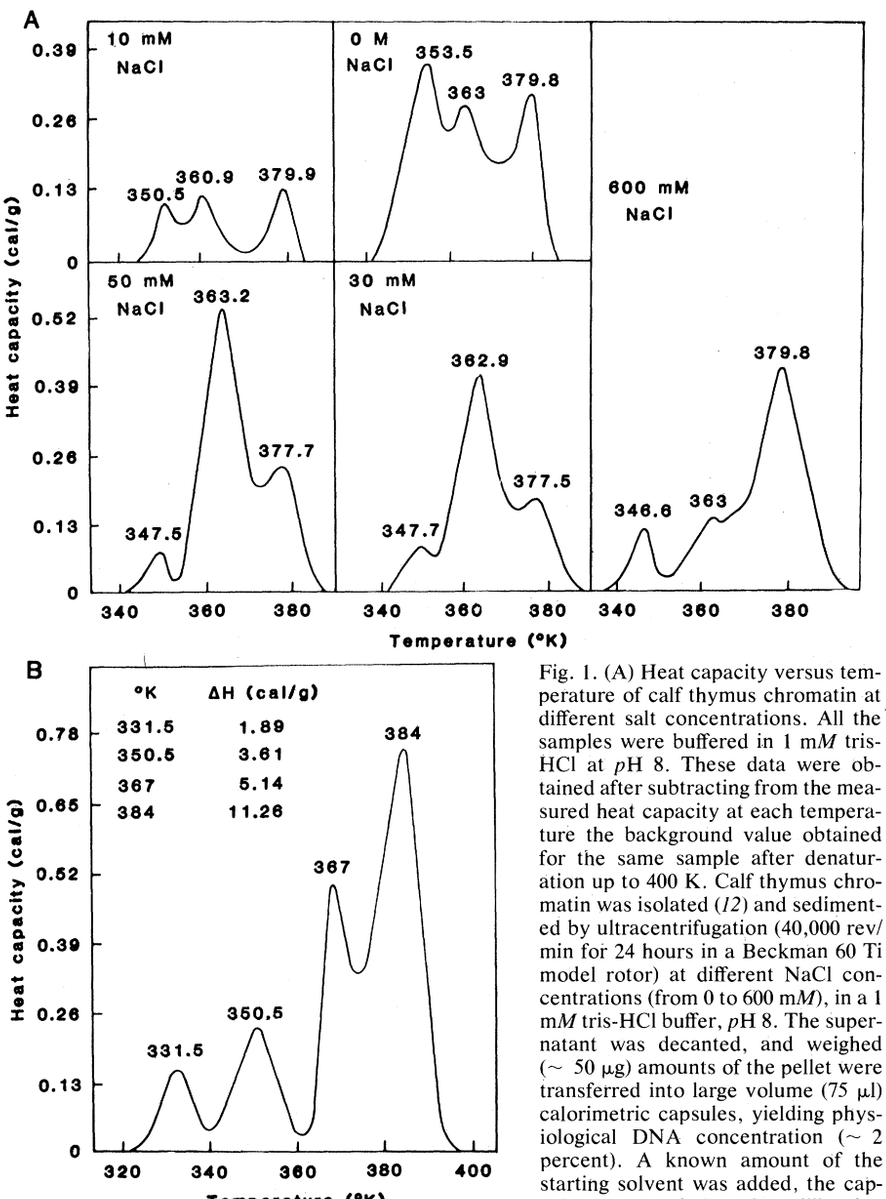

Fig. 1. (A) Heat capacity versus temperature of calf thymus chromatin at different salt concentrations. All the samples were buffered in 1 m*M* tris-HCl at *p*H 8. These data were obtained after subtracting from the measured heat capacity at each temperature the background value obtained for the same sample after denaturation up to 400 K. Calf thymus chromatin was isolated (*12*) and sedimented by ultracentrifugation (40,000 rev/min for 24 hours in a Beckman 60 Ti model rotor) at different NaCl concentrations (from 0 to 600 m*M*), in a 1 m*M* tris-HCl buffer, *p*H 8. The supernatant was decanted, and weighed (~ 50 μg) amounts of the pellet were transferred into large volume (75 μl) calorimetric capsules, yielding physiological DNA concentration (~ 2 percent). A known amount of the starting solvent was added, the capsules were sealed, and equilibration was achieved by keeping the system at 5°C for 5 hours. The DNA content of chromatin was determined spectroscopically. Transition enthalpies were obtained from the areas of the thermograms, according to the standard formula $\Delta H = (K \times R \times A)/(W \times S)$, where ΔH is the enthalpy change expressed in calories per gram of DNA, W is the weight of DNA in milligrams, R is the sensitivity range in millicalories per second per millimeter, S is the chart speed in millimeters per second, and A is the area of the thermal peak in square millimeters. The instrument calibration constant K was found to be equal to 1 under our experimental conditions. A simple instrument was designed to manipulate pellets having different physical properties. At low salt concentration, the material is a swollen, viscous gel, but above 50 m*M*, it becomes thick and rubber-like. The instrument consists of a stainless steel hollow punch, bearing a central plunger; the external body has a sharp tip, its external diameter (0.5 cm) being slightly smaller than the opening of the capsules. With the plunger raised, the soft gels are layered on a clean glass surface and sampled by gently pressing the hollow punch on them. (B) Heat capacity versus temperature of intact liver nuclei from untreated rat, isolated as described (*9, 12*). Intact rat liver nuclei were studied under physiological conditions and harvested at 25,000 rev/min for 3 hours (Beckman SV 50 L) (*12*). The average range of ratios by weight among DNA, RNA, and protein for these nuclei preparations was about 1:0.2:3.0 (*12*).

for transition III at 1 m*M* tris-HCl coincides with the temperature at which a dramatic increase in absorbance and a decrease in molar ellipticity occur simultaneously at 272 nm (Table 1 and Fig. 1). This combined with the pronounced salt dependence of the enthalpy (Fig. 2) points to a possible assignment of transition III to the DNA helix–coil transition, since it is stabilized by histone octamers in the nucleofilament.

A similar assignment for the 10 to 600 m*M* NaCl calorimetric profiles is compatible with the circular dichroism and absorbancy thermal profiles, which show that at ionic strengths greater than 7 m*M*, the helix-coil transition occurs at temperatures above 368°K. In the range 10 to 600 m*M* NaCl, DNA denaturation indeed cannot be monitored with standard optical techniques (*6, 10*), whereas DNA superhelix-helix and protein denaturation can be so monitored; their spectroscopically observed transitions occur in the temperature range of calorimetric transitions II and I, respectively.

Intact nuclei from the same rat liver cells (Fig. 1) display a highly reproducible transition (0) at a temperature close to 332 K (59°C) which is systematically absent in the isolated chromatin. In addition, the transition at 346 to 353 K (transition I), which at 10 to 600 m*M* yielded a constant low value of the enthalpy of transition in the isolated chromatin (see Figs. 1 and 2), dramatically increased by a factor of 4 in the intact nuclei. As indicated by circular dichroism melting curves at 223 nm, transition I appears to be related to the melting of macromolecules (such as proteins) bound to chromatin, but present in substantially increased amounts in nuclei. As expected from the equivalent NaCl normality within the sedimented nuclei, which was about 100 m*M* as independently evaluated by complex dielectric constant measurements (*12*), the melting enthalpy increased for the transition at 380 K (transition III), whereas it had a value similar to that of the 50 m*M* isolated chromatin for the transition at 360 to 367 K (transition II).

This is exactly what was predicted from the polyelectrolyte theory (*11*) for the ionic strength dependence of a quaternary chromatin structure (and stability) under the assumption that the fraction (0.30) of DNA phosphate charges neutralized by H1 histones is the same in isolated and native nuclear chromatin. The other transition (0), consistently observed at lower temperature (332 K) only in isolated nuclei, could be related to the melting of a quinternary

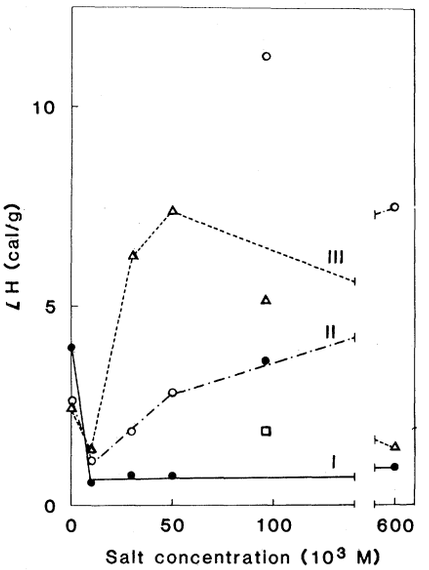

Fig. 2. The dependence of the melting enthalpy, ΔH_m, on NaCl concentration for the chromatin thermal transitions corresponding to the first (I), second (II), and third (III) peaks in the thermal profiles of Fig. 1. The values at 100 m*M* NaCl, equivalent to the ionic strength in native nuclei (*12*), is also plotted for chromatin in situ.

chromatin DNA structure (*5*) present only in situ.

These calorimetric data, which correlate well with viscoelastometric (*13*) and electron microscopic (*12*) data on the same nuclei, point to possibly three successive foldings of DNA in native chromatin, from tertiary (transition III) to quinternary (*1–5*). From pure calorimetric data, no details can be inferred about the specific geometric configuration of these higher order structures, but the number and discrete nature of these thermal transitions are compatible with only two successive packings of nuclear DNA during interphase, behind the nucleosome—one at the quaternary (*2, 3, 12*) and the other at the quinternary (*5, 12*) level.

C. Nicolini
National Research Council, University of Genoa, Genoa, Italy, and
Health Sciences Center, Division of Biophysics, Temple University, Philadelphia, Pennsylvania 19140
V. Trefiletti, B. Cavazza
C. Cuniberti, E. Patrone
Center for Physicochemical Study of Macromolecules, National Research Council of Italy, Rome
P. Carlo
G. Brambilla
Institute of Pharmacology, University of Genoa

References and Notes

1. G. Felsenfeld, *Nature (London)* **271**, 115 (1978).
2. J. Finch and A. Klug, *Proc. Natl. Acad. Sci. U.S.A.* **73**, 1897 (1976).
3. C. Nicolini and F. Kendall, *Physiol. Chem. Phys.* **9**, 265 (1977).
4. J. Sedat and L. Manuelidis, *Cold Spring Harbor Symp. Quant. Biol.* **42**, 331 (1977).
5. C. Nicolini, *J. Submicrosc. Cytol.* **12**, 475 (1980).
6. K. E. Van Holde *et al.*, in *Chromatin Structure and Function*, C. Nicolini, Ed. (Plenum, New York, 1979), pp. 389–412.
7. A. Fulmer and G. Fasman, *Biopolymers* **18**, 2875 (1979).
8. P. Miller, F. Kendall, C. Nicolini, *Nucleic Acids Res.* **3**, 1875 (1976).
9. P. Miller, W. Linden, C. Z. Nicolini, *Naturforschung* **34**, 442 (1979).
10. T. Dolby, T. Borun, S. Gilmour, A. Cohen, A. Zweidler, P. Miller, C. Nicolini, *Biochemistry* **18**, 1333 (1979).
11. A. Belmont and C. Nicolini, *J. Theor. Biol.* **90**, 169 (1981).
12. C. Nicolini *et al.*, in *Chemical Carcinogenesis*, C. Nicolini, Ed. (Plenum, New York, 1982), pp. 381–434.
13. C. Nicolini, P. Carolo, A. Martelli, R. Finollo, F. Bignone, G. Brambilla, *J. Mol. Biol.* **161**, 1 (1982).

29 September 1982

Uphill Sodium Transport Driven by an Inward Calcium Gradient in Heart Muscle

Abstract. *Heart cells were loaded with sodium by treatment with toxic doses of acetyl strophanthidin. After this treatment, an increase in extracellular calcium resulted in a transient net outward sodium flux against its electrochemical gradient and in net cellular uptake of calcium. It is concluded that the free energy for the net outward sodium movement was derived from the increased calcium gradient and that these ion movements took place through the sodium-calcium exchange. While in the normal physiological state the sodium-calcium exchange produces calcium extrusion from the cell, these experiments demonstrate its reversibility.*

There exists, in a variety of cells, a coupled exchange of sodium for calcium (*1*). This exchange is thought to provide a mechanism for the outward transport of calcium that enters cardiac cells by electrodiffusion (*2*). Moreover, the immediate energy source for this calcium transport is thought to be the large electrochemical gradient for sodium. It is conceivable that sodium-calcium exchange can reverse its direction and transport sodium out of the cell (against